Sports Medicine and Health Science 8 (2026) 163–171

Contents lists available at ScienceDirect

Sports Medicine and Health Science

journal homepage: www.keaipublishing.com/smhs

Original Article

Comparison of maximal strength, muscle morphology, and motor unit recruitment and firing rate patterns of the abductor digiti minimi in normal-fat and over-fat males

Lyric D. Richardson [a], Alex A. Olmos [b], Allen L. Redinger [a], Stephanie A. Sontag [c], Sunggun Jeon [d], Brenden L. Roth [a], Emma G. High [a], Breanne S. Baker [a], Jerome Hauselle [e], Michael A. Trevino [a,*]

[a] *Department of Kinesiology, Applied Health, and Recreation, Oklahoma State University, Stillwater, OK, 74075, USA*
[b] *Department of Molecular Biology and Chemistry, Christopher Newport University, Newport News, VA, 23606, USA*
[c] *School of Kinesiology, Louisiana State University, Baton Rouge, LA, 70803, USA*
[d] *Department of Health and Human Performance, Northwestern State University, Natchitoches, LA, 71497, USA*
[e] *School of Mechanical & Aerospace Engineering, Oklahoma State University, Stillwater, USA*

ARTICLE INFO

Keywords:
Abductor digiti minimi
Body fat
Electromyography
Motor unit
Ultrasonography

ABSTRACT

Purpose: This study examined potential differences in strength, muscle morphology, and motor unit (MU) behavior of the abductor digiti minimi (ADM) between normal-fat (NF) and over-fat (OF) males.
Methods: Dual-energy X-ray absorptiometry assessed percent body fat (%BF). Ultrasonography determined muscle cross-sectional area (CSA), echo intensity (EI), and subcutaneous fat (sFAT). MU behavior was assessed during isometric muscle actions at 50% of maximal voluntary contraction (MVC) by analyzing the *y*-intercepts and slopes for the MU action potential amplitude ($MUAP_{AMP}$) vs. recruitment threshold (RT) relationships, the *A* and *B* terms for the mean firing rate (MFR) vs. RT relationships, and normalized electromyographic amplitude (N-EMG_{RMS}). MU firing times and waveforms were validated with reconstruct-and-test and spike trigger average procedures.
Results: %BF was greater for OF (25.70% ± 5.40%) than NF (16.50% ± 2.20%; $p < 0.001$). MVC was greater for NF (27.13 ± 7.16) N than OF ([19.89 ± 4.96] N; $p = 0.014$). CSA was greater for NF (2.48 ± 0.39) cm^2 than OF ([1.95 ± 0.47] cm^2; $p = 0.011$). The *y*-intercepts for the $MUAP_{AMP}$ vs. RT relationships were greater for NF (0.283 ± 0.254) mV than OF ([-0.221 ± 0.659] mV; $p = 0.004$). The *B* terms for the MFR vs. RT relationships were greater for NF (−0.024 ± 0.003) pps/%MVC than OF ([-0.031 ± 0.009] pps/%MVC; $p = 0.038$). N-EMG_{RMS} was similar between groups ($p = 0.463$).
Conclusion: Maximal strength, muscle size, and MU recruitment and firing rate patterns for a non-weight bearing muscle differed between normal-fat and over-fat males.

1. Introduction

Obesity is a metabolic health condition characterized by an excess accumulation of body fat, which is accompanied by cardiovascular disease, diabetes mellitus, hypertension, and mortality.[1,2] Additionally, increased body fat is associated with deleterious effects on functional performance.[3] It is suggested that weight gain starts an undesirable cycle that decreases physical performance, results in physical limitations, leads to less physical activity, and results in further weight gain and performance decrements.[4]

Despite previous research investigating the influence of adiposity on neuromuscular function,[5] there is minimal research regarding body fat and motor unit (MU) properties. All three studies that examined MU behavior between normal-fat (NF) and over-fat (OF) individuals included participants aged 7–10 year-old.[6–8] Currently, there is no information regarding MU behavior for NF and OF adults. It is possible MU behavior may differ between these groups due to contrasting activity patterns.[9]

Therefore, this study examined maximal strength, muscle morphology, and MU recruitment and firing rate patterns of the abductor digiti minimi (ADM) for NF and OF males during an isometric 50% maximal voluntary contraction (MVC). The ADM was selected as it does

* Corresponding author. Applied Neuromuscular Physiology Laboratory Department of Health and Human Performance Oklahoma State University, 191 CRC Stillwater, OK, 74074, USA.
E-mail address: michael.a.trevino@okstate.edu (M.A. Trevino).

Peer review under the responsibility of Editorial Board of Sports Medicine and Health Science

https://doi.org/10.1016/j.smhs.2025.02.009
Received 14 October 2024; Received in revised form 11 February 2025; Accepted 25 February 2025
Available online 27 February 2025

Abbreviations:

MU	motor unit
ADM	abductor digiti minimi
NF	normal-fat
OF	over-fat
%BF	body fat
CSA	cross-sectional area
EI	echo intensity
sFAT	subcutaneous fat
EMG	electromyographic
DXA	dual-energy X-ray absorptiometry
B-mode	portable brightness-mode
MVC	maximal voluntary contraction
$MUAP_{AMP}$	motor unit action potential amplitude
RT	recruitment threshold
MFR	mean firing rate
N-EMG_{RMS}	normalized electromyographic amplitude
$MUAP_{DUR}$	motor unit action potential duration

not support a significant portion of body mass, which may act as a chronic training stimulus,[10] while also minimizing the potential influence of subcutaneous fat (sFAT) on electromyographic (EMG) signal filtering. We hypothesize the NF will have greater MVC and anatomical muscle cross-sectional area (CSA) of the ADM, resulting in different MU recruitment and firing rate patterns.

2. Methods

2.1. Ethical approval

This study was performed in line with the policy statement regarding the use of human subjects by the Helsinki Declaration of 1975, as revised in 2013. The University's institutional review board for human subject's research approved this study, and written consent was obtained prior to participation (protocol number: IRB-20-464-STW).

2.2. Study design

This study utilized a between-group design, where participants reported to the laboratory on two occasions, separated by a minimum of two days, but no more than 7 days. Visit 1 consisted of dual-energy X-ray absorptiometry (DXA) to obtain %BF, and ultrasonography (US) of the ADM to obtain anatomical muscle CSA, echo intensity (EI), and sFAT thickness. Participants were also familiarized with strength testing measurements of the ADM. During the second visit, participants performed MVCs of the ADM followed by a submaximal isometric trapezoidal muscle action at 50% MVC. Surface EMG signals were recorded from the ADM to measure peak EMG amplitude (EMG_{RMS}) during the MVCs, and to calculate normalized EMG_{RMS} (N-EMG_{RMS}) for the 50% submaximal muscle action. Subsequently, surface EMG signals were decomposed to extract the recruitment threshold (RT), mean firing rate (MFR) at the targeted force, motor unit action potential amplitude ($MUAP_{AMP}$), and MUAP duration ($MUAP_{DUR}$) for each observed MU. Participants refrained from any alcohol and caffeine consumption, and strenuous upper-body physical activity for 24 hours (h) and 48 h, respectively (Fig. 1).

2.3. Participants

Twenty-one male adults between 18 and 40 yrs participated in this study. Participants were grouped as NF or OF according to the World Health Organization (NF %BF < 20% < OF %BF).[11,12] Therefore, ten participants were NF (mean ± *SD*; age: [27 ± 5] yrs., height: [177.65 ± 4.48] cm, body mass: [82.41 ± 12.09] kg, %BF: [16.50% ± 2.20%]), whereas eleven were OF (age: [23 ± 3] yrs., height: [176.23 ± 4.59] cm, body mass: [96.91 ± 21.05] kg, %BF: 25.70% ± 5.40%). Participants for the NF reported (3 ± 3) h and (4 ± 3) h of endurance- and resistance-training per week, whereas the OF reported (1 ± 2) h and (3 ± 4) h of endurance- and resistance-training per week. Participants reported no ongoing neuromuscular, metabolic, or cardiovascular diseases, or previous injuries to the hand. Based on Colim,[13] power calculation software (G*power 3.1.9.7, Heinrich-Heine- Universität Düsseldorf, Dusseldorf, Germany) indicated that at least 12 participants were necessary for a possible difference in neuromuscular behavior between NF and OF adults.

2.4. Body fat and muscle morphological measures

2.4.1. DXA scans

Participants arrived in metal-free athletic clothing and engaged in normal hydration habits. Height (cm) and body mass (kg) were collected via a stadiometer (500 KL-BT, Health O Meter® Professional., McCook, IL, USA). Participants then provided a urine sample and researchers confirmed proper hydration (1.004–1.028 urine specific gravity) using digital refractometry (MISCO #PA201, Solon, OH). A Hologic Horizon A model DXA (Apex Software V 5.6.1.2 rev 009, Hologic Inc., Marlborough, MA, USA) was used to complete a single total-body scan with participants positioned supine as previously detailed[14,15] to stratify individuals as either NF (≤ 20% BF) or OF (> 20% BF). All scans were completed by the same Hologic-certified DXA operators, and respective coefficient of variations of 0.80%, 0.48%, and 0.95% for bone, lean, and adipose tissue have previously been reported by the researchers.[16] All data were extracted and organized using DXA[2] software.[17]

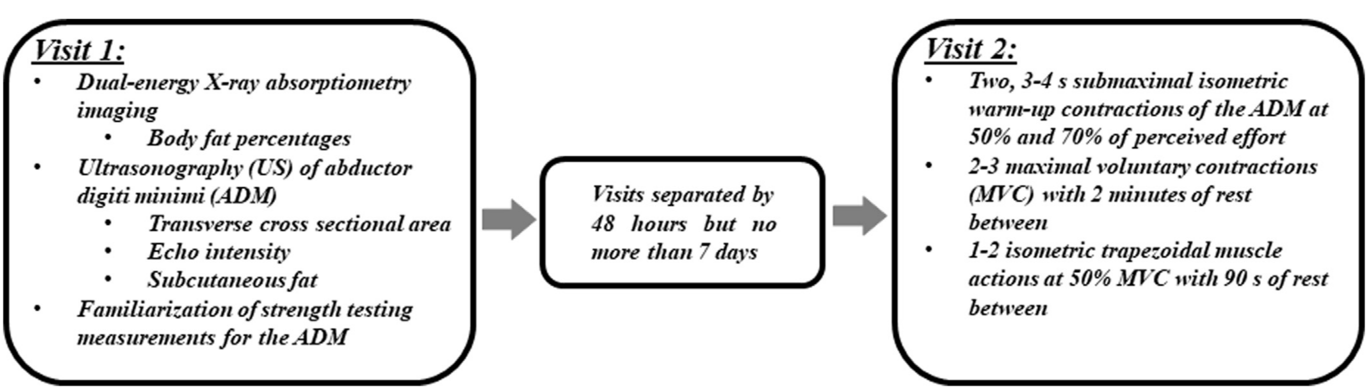

Fig. 1. Time line of the experimental study design.

2.4.2. Ultrasonography

Anatomical muscle CSA and EI of the ADM, and sFAT overlying the ADM were measured via a portable brightness-mode (B-mode) Logiq® S8 ultrasound device (LOGIQ S8 GE Ultrasound System; GE Healthcare, Milwaukee, WI, USA) with a 4 MHz–15 MHz multi frequency linear array probe (ML6-15-D; 50 mm field of view; GE Healthcare system). Scan depth was set to 4, gain was 50 dB, and transducer frequency was 12 MHz to optimize image quality, and was consistent across all participants. During testing, participants rested their arm supine on an examination table in a relaxed position. Following 10 minutes (min) of rest to allow fluid settling,[7,8,18] a generous amount of water-soluble transmission gel was applied to the skin to reduce possible near field artifacts and enhance acoustic coupling, and the ADM was measured at the proximal third of the fifth metacarpal. Transverse CSA images were captured at the ulnar side of the hand, and minimal pressure was applied to the ADM with the probe to limit compression of sFAT and the muscle.[19] All ultrasound imaging analyses were performed with ImageJ software (National Institutes of Health, Bethesda, MD). Each image was scaled from pixels to cm using the straight-line function. For CSA (cm^2), the ADM was outlined using the polygon function, and care was taken to exclude the surrounding fascia during the measurement. Muscle tissue composition was evaluated with EI from the same area selected for CSA determination. Raw EI was calculated with gray-scale analysis using standard the histogram function, and was corrected for sFAT.[20,21] sFAT was quantified as the distance between the skin and the superficial aponeurosis of the ADM at the centermost point of the muscle.

2.5. Isometric strength testing

Participants were seated upright with their right forearm pronated and positioned on a table. The forearm, wrist, and thumb were immobilized with a wrist brace, and the thumb was resisted with a wooden stopper that would allow for approximately an 80° angle between digits one and two. Digits 2–4 were secured with a Velcro strap, while isolating the fifth digit for isometric finger abduction. Force during the muscle actions of the ADM was measured during abduction of the fifth digit against a small flat piece of metal connected to a force transducer (MB-100; Interface, Inc., Scottsdale, AZ). The force signals were amplified (500 ×) with a load cell amplifier (Forza, OT Bioelettronica, Torino, IT). For the experimental visit, participants performed two, 3–4 seconds (s) held submaximal isometric warm-up contractions at 50% and 70% of perceived maximal effort, followed by two to three MVCs, each separated by 2 min of rest. During the MVCs, participants were instructed to "push out as hard and as fast as possible" and sustain the maximal contraction for 3–4 s. Verbal encouragement was provided during each attempt. The MVC with the highest force (N) averaged over a 0.25 s epoch determined maximal strength and the force level for the submaximal contractions. Following 2 min of rest, participants performed an isometric trapezoidal muscle action at 50% MVC. It has been reported that targeted force trajectory compliance greatly influences the group analysis, such as not

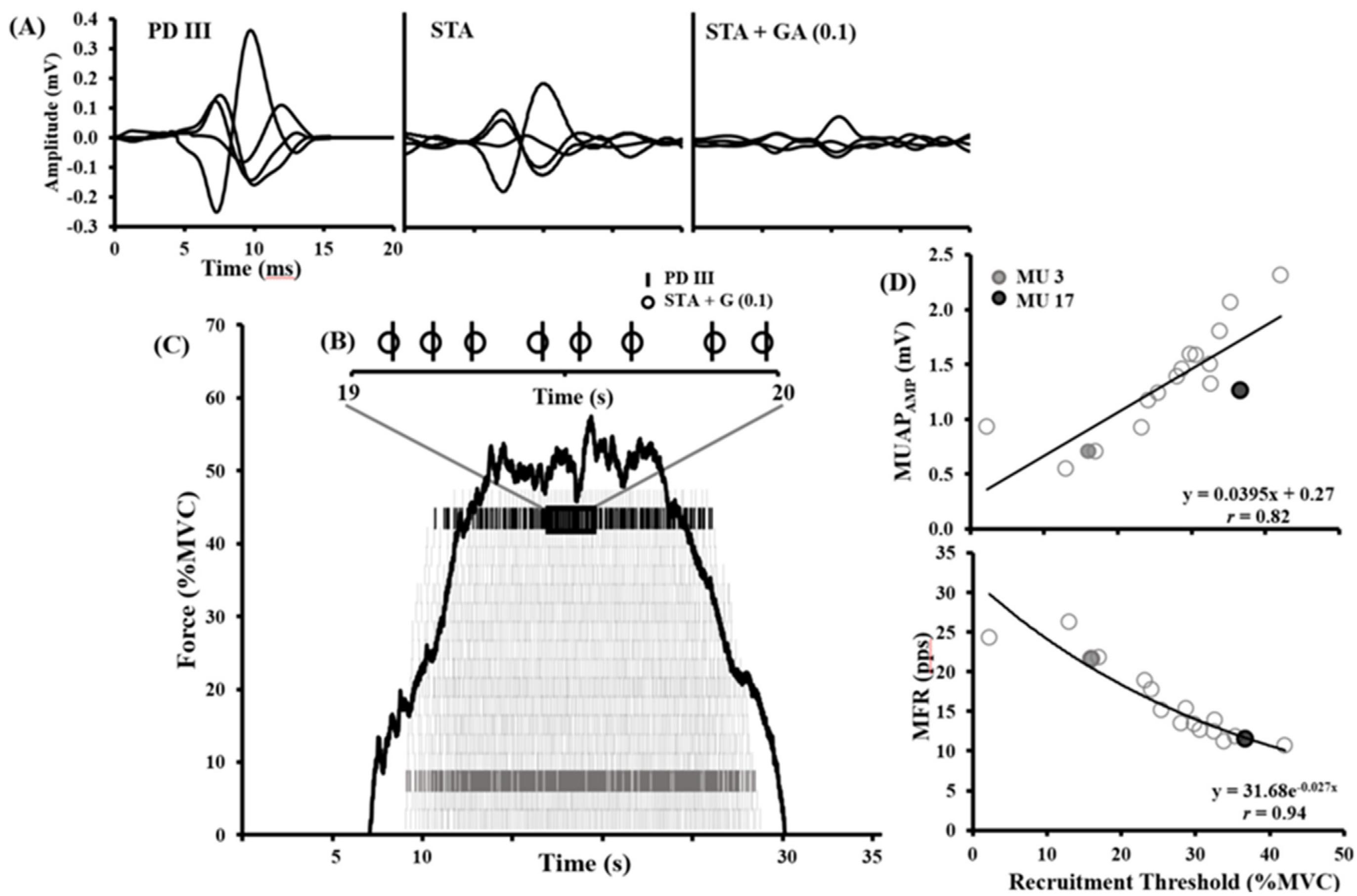

Fig. 2. (A) The motor unit action potential (MUAP) waveforms decomposed from the precision decomposition (PD) III algorithm, the user created waveforms from the raw electromyographic signals by spike trigger averaging (STA), and the recreation of the waveforms via STA with the addition of Gaussian noise (0.1 * *SD* of the interspike intervals) added to the firing times (STA + G [0.1]). (B) The correct firing times from the PD III algorithm (vertical marks), and the firing times with additional Gaussian noise (STA + G [0.1], circles) for 1 s of steady force. (C) An example of the force tracing overlaid onto the correct firing times of 18 detected motor units (MUs) from the abductor digiti minimi during the isometric trapezoidal contraction at 50% maximal voluntary contraction (MVC) for one participant with MUs 3 and 17 indicated in bold. (D) The MUAP amplitude ($MUAP_{AMP}$, mV) and mean firing rate (MFR, pulses per second [pps]) vs. recruitment threshold (expressed as % MVC) relationships with the calculated linear or exponential equation for one participant.

reaching/sustaining force results in firing rates that are falsely indicative of a lower level of input excitation.[22] Therefore, 50% MVC was selected for the current study as pilot testing indicated that was highest contraction intensity where all participants could complete targeted force trajectory with sufficient compliance. The isometric trapezoidal muscle action trajectory consisted of a 5 s baseline, a force increase at a rate of 10% MVC/s to the desired force level, a 12 s steady force segment, and a decrease of 10% MVC/s back to baseline. Therefore, the duration of the 50% MVC lasted 22 s (Fig. 2A). During each isometric trapezoidal muscle action, participants were instructed to maintain their force output as accurately as possible to the target force presented digitally in real time on a computer monitor. A second attempt was given after 90 s if a participant was unable to sustain their target force output on the first trial.

The force signals during the MVCs were recorded with a voltage input module (model: 9215, National Instruments, Austin, TX) that was interfaced to a compact data acquisition chassis (Model: 9174, National Instruments, Austin, TX) at 2 kHz, and were low-pass filtered with a 10-Hz cutoff (fourth-order Butterworth). For the isometric trapezoidal muscle actions, force was recorded at 20 kHz with a Bagnoli 16 channel EMG system (Delsys Inc., Boston, MA USA) and was low-pass filtered with a 10-Hz cutoff (fourth-order Butterworth filter). Offline processing was performed in custom-written LabVIEW software version 20 (National Instruments, Inc., Austin, TX, USA).

2.6. Electromyography

2.6.1. Electromyographic recording

A 5-pin surface array sensor (Delsys, Boston, MA) recorded surface EMG signals from the ADM during the MVCs and trapezoidal muscle actions. Each pin has a 0.5 mm diameter and are positioned at the corners of a 5 mm × 5 mm square, with the fifth pin in the center. Prior to sensor placement, the surface of the skin was prepared by shaving, removing superficial dead skin with adhesive tape, and sterilized with alcohol to remove skin contaminants. The sensor was placed over the muscle belly of the ADM and a reference electrode was placed over the seventh cervical vertebrae at the neck. The signals recorded from the four pairs of the sensor electrodes were differentially amplified and filtered with a bandwidth of 20 Hz to 9.5 kHz. The signals were sampled at 20 kHz and stored for subsequent decomposition and analysis.

2.6.2. EMG decomposition

For further detailed information regarding signal processing of EMG signals, refer to De Luca et al.[23] and Nawab et al.[24] Action potentials were extracted into firing events of single MUs from the four separate EMG signals via the Precision Decomposition (PD) III algorithm (version 4.1.1.3) as described by De Luca et al.[23] This algorithm decomposes EMG signals into MU action potential trains and provides a distinctive waveform for each EMG channel. The accuracy of the decomposed firing instances was initially tested with the reconstruct-and-test procedure,[24] and only MUs with $>$ 90% accuracy were used for further analysis. Additionally, secondary spike trigger averaging (STA) procedures were performed to validate the firing times and action potential waveforms created via the PD III algorithm. The derived firing times from the PD III algorithm were used to STA the 4 raw EMG signals.[25–30] MUs demonstrating high correlations ($r \geq 0.7$) across the 4 channels between the PD III algorithm and the STA-derived action potential waveforms and a coefficient of variation for the STA derived peak to peak amplitudes < 0.3 across time were selected for analysis.[25,29,30] The average correlation between the STA and the PD III created waveforms was (0.881 ± 0.079). Seemingly valid MUAP waveforms may be created from trigger events that don't correspond with MU discharge times.[31] Therefore, Gaussian noise set at 10% of the standard deviation for the interspike interval (72 ms) was added to the discharge times for each MU.[25,28–30,32] Subsequently, correlations were performed between the MUAP waveforms created from the raw EMG signals with the small amount of noise (7.2 ms shift) added to the firing times and the MUAP waveforms triggered with the PD III algorithm derived firing times.[28–30] The change in firing times with Gaussian noise is a function of the discharge rate of the MUs. For example, the shift in firing times for each MU with the STA + noise procedure is dependent on muscle tested, recruitment threshold, and contraction intensity (level of input excitation). Such as the shifts in firing times will be less for smaller-compared to larger muscles, lower-compared to higher-threshold MUs, and for a respective MU during higher-compared to lower-contraction intensities due to greater firing rates. Adding a small amount of noise to the firing times should decrease the correlation between MUAP waveforms derived from the PD III algorithm and the STA procedures.[28–30] Indeed, the correlations performed on the MUAP waveforms created from the raw EMG signals with Gaussian noise with the PD III MUAP waveforms were lower ($r = 0.641 \pm 0.109$). Additionally, peak-to-peak amplitudes of the STA MUAP waveforms were compared to the MUAP waveforms derived from the firing times with the addition of Gaussian noise. The peak-to-peak amplitudes derived from the firing times with Gaussian noise should decrease if no true action potential waveforms are consistently present (Fig. 2A). A significant decrease in the r values and the average MU peak-to-peak amplitude due to the addition of Gaussian noise to the firing times would suggest that the PD III algorithm provided valid firing times and action potential waveforms during the surface EMG signal decomposition procedure.

For each MU, four parameters were extracted from the firing rate data: (1) RT (expressed as relative to MVC [%MVC]), (2) MFR at the targeted force level (pps), (3) $MUAP_{AMP}$ [(expressed in millivolts [mV]), and (4) $MUAP_{DUR}$ (expressed in milliseconds [ms]). The RT was calculated as the average force from a 0.10 ms epoch of force that began at the first discharge of the MU.[26,29,33] The MFR was calculated as the inverse of the average interspike intervals during the first 8 s of the steady force segment of the isometric trapezoidal template. The $MUAP_{AMP}$ was calculated as the average peak-to-peak amplitude (mV) of each of the four action potential waveforms, whereas $MUAP_{DUR}$ was calculated as the average peak-to-peak duration of each of the four action potential waveforms.

2.6.3. Normalized electromyography

Channel 1 of the four differential EMG signals from the 5-pin sensor was selected for time-domain analysis[6,29,30] and used for the subsequent amplitude analyses. The EMG signals were band-pass filtered (zero-phase fourth-order Butterworth) at 10 Hz–500 Hz, and peak EMG amplitude was calculated as the average root mean square (RMS) value from the greatest 0.25 s peak force epoch during the MVC. The average EMG_{RMS} value during the 8 s epoch analyzed for MFR calculation during the steady force segment of the 50% isometric trapezoidal muscle action was normalized (N-EMG_{RMS}) [%max] to peak EMG_{RMS} during the MVCs. Data were stored on a personal computer (Dell Optiplex 7040; Dell, Inc., Round Rock, TX, USA) and processed offline using a custom-written LabVIEW software version 22 (National Instruments, Inc., Austin, TX, USA).

2.7. Statistical analysis

Linear regressions were performed on the $MUAP_{AMP}$ and $MUAP_{DUR}$ vs. RT relationships[34–36] for each subject with the y-intercepts and slopes used for statistical analysis. Exponential models were applied to each individual's MFR vs. RT relationship to yield an A and B term for statistical analysis (Fig. 2D). The F test for the change in R^2, as described by Pedhazur,[37] indicated the majority of relationships (16 of 21 [76%]) were better fit with exponential ($r = -0.920 \pm 0.050$) rather than linear models ($r = -0.906 \pm 0.056$). For the MFR vs. RT model, $MFR = Ae^{B(RT)}$, where A is the theoretical MFR for a MU recruited at 0% MVC, e is the natural constant, and the B term represents the rate of decay for MFR with increments in RT.

To examine potential differences between groups, independent samples *t*-tests were performed on %BF, BMI, MVC, CSA, EI, sFAT, N-EMG_{RMS}, the *y*-intercepts and slopes for the $MUAP_{AMP}$ and $MUAP_{DUR}$ vs. RT relationships, and the *A* and *B* terms for the MFR vs. RT relationships. To determine the validity of the MUAP waveforms detected from the additional STA procedures, a Fisher's *r* to *z* transformation[38] was performed for each subject on the correlation coefficient values between the MUAP waveforms derived from the PD III algorithm and the STA procedures, and the waveforms derived from the PD III algorithm and the STA procedure with the addition of Gaussian noise added to the firing times. The *z*-scores were compared using a dependent samples *t*-test. Additionally, a dependent samples *t*-test examined potential differences in $MUAP_{AMPS}$ between the peak-to-peak amplitudes of the STA MUAP waveforms and the MUAP waveforms with Gaussian noise added to the firing times. A significant decrease in the *z*-scores and the average MU peak-to-peak amplitude due to the addition of Gaussian noise to the firing times suggests that the PD III algorithm provided valid firing times and action potential waveforms.[26,29,30]

Greenhouse-Geisser corrections were applied when sphericity was not met according to Maulchy's Test. The level of significance was set at $p \leq 0.05$. Effect sizes for interactions were estimated using partial eta squared and were classified as small (0.01–0.06), medium (0.06–0.14), or large (> 0.14). Effect sizes for between comparisons were estimated using Hedge's *g* and were classified as minimal (0–0.2), small (0.2–0.5), medium (0.5–0.8), or large (> 0.8). All statistical analyses were performed using SPSS 20 (IBM Corporation, Armonk, New York, USA).

3. Results

3.1. Body composition, ultrasonography, and voluntary strength

Table 1 contains a summary of the independent samples *t*-tests and means ± *SD*s for body composition, ultrasonography, and voluntary strength data.

Independent samples *t*-tests indicated the OF had significantly greater %BF ($p < 0.001$; $g = 2.21$) and BMI ($p = 0.050$; $g = 0.92$). The NF had greater CSA ($p = 0.011$; $g = 1.19$) and MVC ($p = 0.014$; $g = 1.14$). There were no differences between groups for EI ($p = 0.366$; $g = 0.39$) or sFAT ($p = 0.547$; $g = 0.26$).

3.2. Motor unit data

Eleven MUs were rejected following the STA procedures (NF = 2 MUs; OF = 9 MUs), resulting in the analysis of 415 total MUs (NF = 193 MUs; OF = 222 MUs) (NF = 19 ± 7; OF = 20 ± 6 per contraction). The number of MUs and RT ranges for the 50% MVC are listed in Table 2. All (100%) $MUAP_{AMP}$ ($r = 0.0733$–0.977) and MFR vs. RT relationships ($r = -0.749$ to -0.983) were significant ($p \leq 0.050$). Adding a small amount of Gaussian noise to the PD III algorithm derived firing times deteriorated the MUAP waveform, such as a significant decrease in peak-to-peak amplitudes ($p < 0.001$; [0.657 ± 0.392] mV to [0.009 ± 0.005] mV) (Fig. 2A) and the *z*-scores calculated from the correlation coefficients ($p < 0.001$; [1.475 ± 0.347] to [0.783 ± 0.196]) with minor shifts in firing times.

Table 1
Participant body composition, voluntary strength, and ultrasonography data.

	NF	OF	*P Value*	Hedges' *g*
%BF	16.50 ± 2.20	25.70 ± 5.40	<0.001*	2.21
BMI, kg/m^2	26.15 ± 4.05	31.17 ± 6.50	0.050*	0.92
MVC force, N	27.13 ± 7.16	19.89 ± 4.96	0.014*	1.18
EI, AU	27.25 ± 9.82	24.16 ± 4.88	0.385	0.40
CSA, cm^2	2.48 ± 0.39	1.95 ± 0.47	0.011*	1.22
sFAT, mm	0.07 ± 0.07	0.90 ± 0.05	0.547	0.06

Data are means ± *SD* for percent body fat (%BF), body mass index (BMI), maximal voluntary contraction (MVC) force, echo intensity (EI), cross-sectional area (CSA), and subcutaneous fat (sFAT) in normal-fat (NF) and over-fat (OF) groups, *p* values and Hedge's *g* effect sizes. AU, arbitrary units. *$p \leq 0.05$ indicates significance difference between NF and OF.

Table 2
Number of motor units (MUs) and recruitment threshold (RT) ranges (expressed at % of maximal strength) during the 50 % maximal voluntary contraction for the normal-fat (NF) and over-fat (OF) participants.

	NF		OF	
	MUs	RT range	MUs	RT range
Mean	19	3.54–38.85	20	7.05–37.72
SD	7	3.15–6.26	6	3.60–4.06

3.3. $MUAP_{AMP}$ vs. RT relationships

The independent samples *t*-tests indicated greater *y*-intercepts ($p = 0.035$; $g = 0.95$) for the NF ([0.283 ± 0.254] mV) compared to the OF ([−0.221 ± 0.659] mV), whereas there were no differences between groups for the slopes ($p = 0.245$; $g = 0.50$). Due to one participant having a *y*-intercept and slope value that was respectively 92 and 3.6 times less and greater than the other participants despite similar recruitment threshold ranges, data were reanalyzed with this participant removed. The subsequent analysis indicated greater *y*-intercepts remained ($p = 0.004$: $g = 1.53$) for the NF ([0.283 ± 0.254] mV) compared to the OF ([−0.024 ± 0.099] mV), while there were still no differences between groups for the slopes ($p = 0.477$; $g = 0.31$) (Fig. 3).

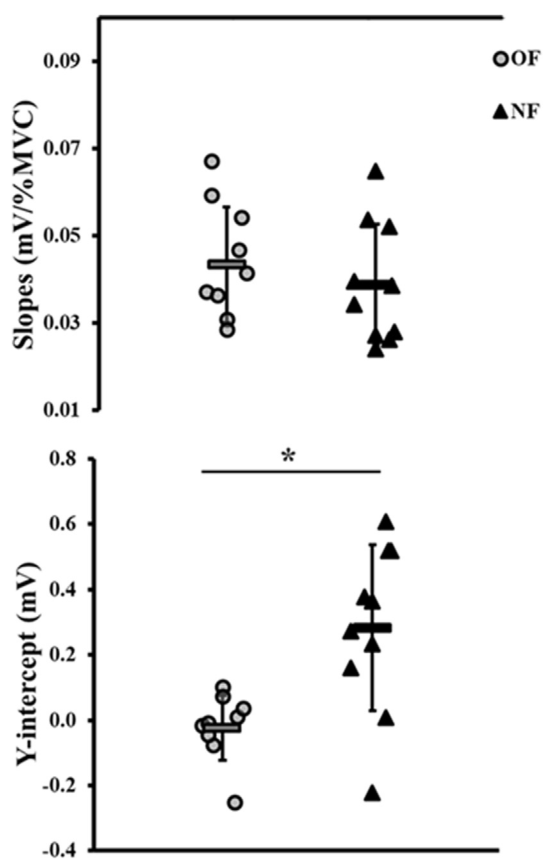

Fig. 3. Plotted individual values and means (± *SD*) for the slopes (top graph) and the *y*-intercepts (bottom graph) from the motor unit action potential amplitude (millivolts [mV]) vs. recruitment threshold (expressed as percent of maximal voluntary contraction [%MVC]) relationships for the over-fat (OF) and normal-fat (NF). * Indicates greater *y*-intercepts for the NF ($p = 0.004$).

3.4. MFR vs. RT relationships

An independent samples *t*-test indicated no differences between groups for the *A* terms ($p = 0.644$: $g = 0.20$). However, an independent samples *t*-test indicated greater *B* terms ($p = 0.038$; $g = 0.94$) for the NF ([−0.024 ± 0.003] pps/%MVC) compared to the OF ([−0.031 ± 0.009] pps/%MVC) (Fig. 4).

3.5. $MUAP_{DUR}$ vs. RT relationships

Only 5 of 21 $MUAP_{DUR}$ vs. RT relationships were significant. Consequently, statistics were not run on the *y*-intercepts or slopes. Conversely, $MUAP_{DUR}$ values were averaged for each subject and analyzed with an independent samples *t*-test. There were no differences ($p = 0.562$; $g = 0.25$) for $MUAP_{DUR}$ between NF and OF.

3.6. Normalized EMG_{RMS}

An independent samples *t*-test indicated no differences between groups for N-EMG_{RMS} ($p = 0.463$: $g = 0.31$) (Fig. 5).

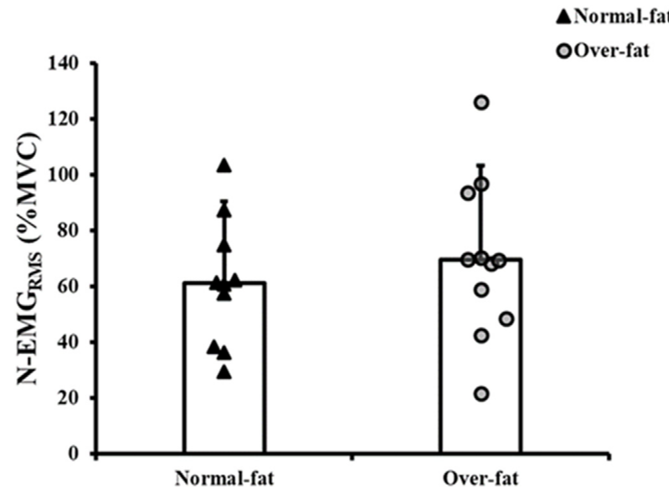

Fig. 5. Plotted individual values and mean (+ *SD*) for normalized electromyographic amplitude (N-EMG_{RMS}) for normal-fat (triangle markers) and over-fat (circle markers).

4. Discussion

As expected, BF% and BMI were greater for the OF compared to the NF. Significant and novel findings between groups include: 1) greater MVC force and CSA of the ADM for the NF, 2) greater *y*-intercepts of the $MUAP_{AMP}$ vs. RT relationships for the NF, and 3) greater *B* terms of the MFR vs. RT relationships for the NF. The lack of differences between groups for $MUAP_{DURS}$ and sFAT overlying the ADM suggests that electrode-MU recording distance or EMG signal filtering did not arbitrarily lead to greater $MUAP_{AMPS}$ for the NF group, respectively. Therefore, maximal strength, muscle size, and MU recruitment and firing rate patterns for the ADM, a muscle that does not support body mass, differed between NF and OF males.

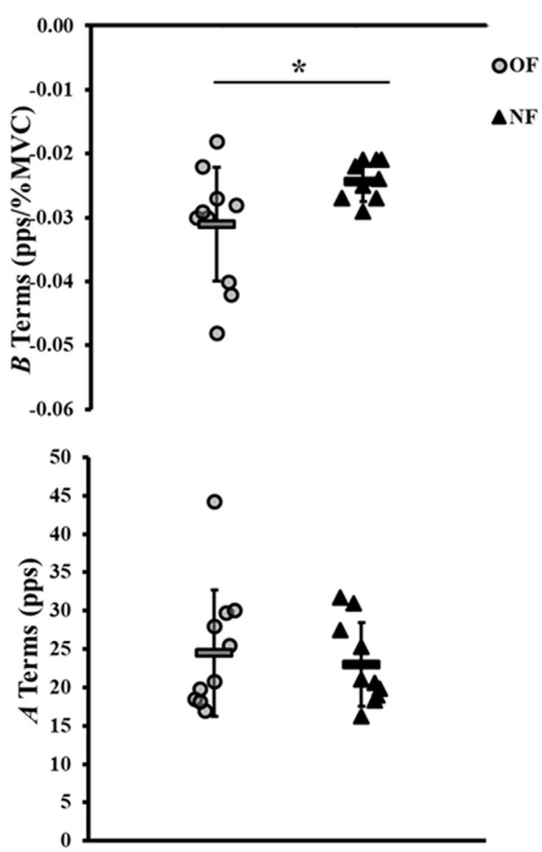

Fig. 4. Plotted individual values and means (± *SD*) for the *B* terms (top graph) and *A* terms (bottom graph) from the mean firing rate (pulses per second [pps]) vs. recruitment threshold relationships (expressed as percent of maximal voluntary contraction [%MVC]) for the over-fat (OF) and normal-fat (NF). * Indicates significantly greater *B* terms for NF ($p = 0.038$).

MVC force for the ADM was greater for the NF than the OF. Conversely, previous studies have reported greater isometric strength of the knee extensors for obese-compared to nonobese-children, with researchers speculating higher body mass for the obese children provided a chronic training stimulus similar to resistance training that increased muscular strength and size.[39–43] However, unlike the knee extensors, the ADM does not support body mass. We are aware of only one study that has investigated maximal strength of a hand muscle between NF and OF individuals. Interestingly, Miller et al.[8] reported no differences for isometric MVC force of the FDI between obese- and nonobese-children. Therefore, the greater MVC force exhibited by the NF for the current study is a novel finding. Although both groups reported similar hours of resistance training per week (4 h vs. 3 h), a greater percentage (70%) of the NF participants reported regularly engaging in resistance training compared to the OF (45%). It is possible the greater MVC for the NF may be the result of training history.

Despite differences in %BF and BMI, ultrasonography revealed similar EI between groups for the ADM. However, CSA for the ADM was greater for the NF. These findings contrast Miller et al.,[8] that reported obese-children possessed poorer muscle quality (greater EI) for the FDI than nonobese-children, while they reported no differences between groups for CSA. It is possible that greater discrepancies in %BF than observed for the current study (9%) are necessary for differences in EI to manifest for an upper body muscle, as the difference for %BF reported between groups for Miller et al.[8] was greater (14%). In support, no differences for EI were previously reported for the biceps brachii between older-compared to younger-adults despite significantly different body fat percentages between groups (~7%).[44] The larger CSA for the NF coupled with similar EI between groups suggests greater contractile tissue for the NF, and may further explain their greater MVCs.[30,45,46]

The *y*-intercepts for the $MUAP_{AMP}$ vs. RT relationships provide insight on the amplitudes of the lowest-threshold MUs, whereas the slopes indicate the rate of change in $MUAP_{AMPS}$ with increments in RTs. The *y*-intercepts were greater for the NF, whereas there were no differences between groups for the slopes. Subsequently, the NF possessed larger lower-threshold MUs (Fig. 6A), which may partially be explained by training-related hypertrophy. Although the NF did not self-report resistance-training specifically targeting the ADM, muscular hypertrophy has

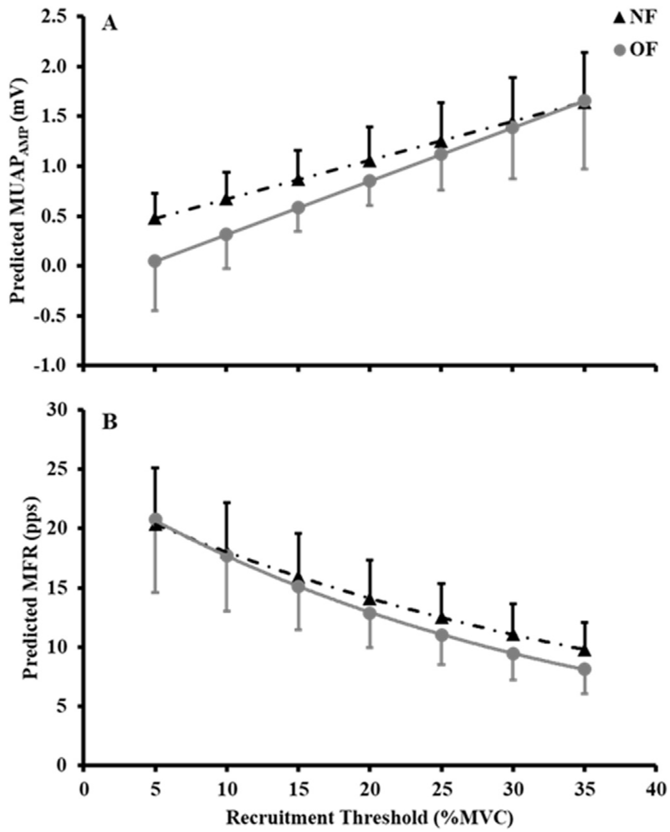

Fig. 6. (Top) Plotted means (*SD*) for the predicted motor unit action potential amplitude ($MUAP_{AMP}$, mV) vs. recruitment threshold (expressed as percent of maximal voluntary contraction [%MVC]) relationship for the normal-fat (triangular markers) and over-fat (circular markers). (Bottom) Plotted means (*SD*) for the predicted mean firing rate (MFR, pulses per second [pps]) vs. recruitment threshold (%MVC) relationship for the normal-fat (triangular markers) and over-fat (circular markers).

been reported following isometric exercise.[47–49] Therefore, the greater $MUAP_{AMPS}$ of the lower-threshold MUs for the NF may be the result of gripping dumb bells, barbells, and machine handles during resistance-training. Additionally, the larger lower-threshold MUs for the NF mirrors the finding for CSA between groups.[44]

For the MFR vs. RT relationships, the *A* terms were similar between groups, whereas the *B* terms were more negative for the OF compared to the NF. Therefore, MFRs of the lowest-threshold MUs at the targeted force were similar; however, MFRs at the targeted force decreased at a greater rate with increments in RTs for the OF (Fig. 6B). Additionally, N-EMG_{RMS} was similar for the NF and OF, suggesting the amount of relative excitation necessary to match the targeted force did not differ between groups. It is suggested that the MU pool is provided a common synaptic input during voluntary efforts, and the firing rates of individual MUs at the targeted force are influenced by their respective physical properties.[9,31,50] For example, inverse relationships have been reported between $MUAP_{AMPS}$ and MU firing rates.[30,36] Although the $MUAP_{AMPS}$ of the lowest-threshold MUs were greater for the NF (Fig. 6A), interestingly, there were no differences in the respective firing rates at the targeted force between groups (Fig. 6B). MU firing rates increases have been reported following isometric training.[51,52] It is possible that the training history for the NF resulted in adaptations to intrinsic motor neuron properties, allowing them to have lower-threshold MUs that were larger than the OF, but also similar firing rates. Of note, the firing rate behavior exhibited by the lower-threshold MUs for the NF would allow for greater mechanical output than the OF, as the amount of force produced by a MU is proportional to its force twitch magnitude and firing rate.[22,29]

The more negative *B* terms for the OF may be due to a greater range in observed $MUAP_{AMPS}$ for the MUs recruited between 5% MVC and 35% MVC (1.61 mV) compared to the NF (1.17 mV) (Graph 6A). Therefore, it is possible the magnitude of MU force twitches changed to a greater degree throughout the recruitment spectrum for the OF, and may explain their greater rate of change (more negative *B* terms) for MFRs at the targeted force with increments in RT. Our findings contradict previous studies that reported no differences in coefficients for MFR vs. RT relationships of the VL[7,53] and FDI[8] between NF and OF children despite differences in $MUAP_{AMPS}$. Nonetheless, this is the first study to report MU firing rate patterns differed in a non-weight bearing muscle between NF and OF adults.

4.1. Limitations

Although the current study provided interesting findings, there is a limitation that should be acknowledged. Despite a familiarization visit, participants were unable to sustain the targeted force of the isometric trapezoidal muscle action for contraction intensities > 50% MVC. It has been reported that the maximum recruitment threshold for the ADM is ~90% MVC[54]; consequently, the highest-threshold MUs were not observed for this study. However, in-depth modeling has suggested that ~70% of all the MUs for the ADM are recruited during a 50% MVC. Therefore, a large portion of the MU pool was recruited during the 50% MVC.

4.2. Implications

The results of this study may suggest implications for occupational performance and/or activities of daily living when OF individuals are completing tasks involving the hand. For example, the loads encountered in everyday life are seldom scaled to the maximal strength of an individual. Maximal strength of the ADM for the NF was ~35% greater than the OF. Therefore, absolute loads will equate to a greater relative intensity for the OF compared to the NF, possibly resulting in a decreased ability to perform submaximal work, occupational tasks, and recreational/daily living activities.

4.3. Conclusion

In conclusion, to our knowledge, this is the first study to collectively examine potential differences in maximal strength, muscle morphology, and MU recruitment and firing rate patterns of the ADM between NF and OF adult males during a moderate-intensity contraction. Muscular size and strength of the ADM were greater for the NF group, contradicting previous research that reported similar CSA and MVC force for the FDI between normal weight- and overweight-children. Lower-threshold MUs were larger for the NF but exhibited similar firing rates compared to the OF, which may explain the greater CSA and MVC force for the NF, respectively. Future research should compare MU behavior between NF and OF adult males at absolute forces/torques, during fatiguing tasks, and examine the effects of a weight loss and resistance training intervention on maximal strength, muscle morphology, and MU characteristics of the ADM in OF individuals.

CRediT authorship contribution statement

Lyric D. Richardson: Writing – review & editing, Writing – original draft, Supervision, Software, Project administration, Methodology, Investigation, Formal analysis, Data curation, Conceptualization. **Alex A. Olmos:** Writing – review & editing, Methodology, Investigation, Formal analysis, Data curation, Conceptualization. **Allen L. Redinger:** Writing – review & editing, Methodology, Investigation, Formal analysis, Data curation, Conceptualization. **Stephanie A. Sontag:** Writing – review & editing, Methodology, Investigation, Formal analysis, Data curation, Conceptualization. **Sunggun Jeon:** Writing – review & editing, Methodology, Investigation, Formal analysis, Data curation, Conceptualization. **Brenden L. Roth:** Writing – review & editing, Methodology, Investigation, Formal analysis, Data curation, Conceptualization. **Emma G. High:** Writing – review & editing, Methodology, Investigation, Formal analysis, Data curation, Conceptualization. **Breanne S. Baker:** Writing – review & editing, Methodology, Investigation, Formal analysis, Data curation, Conceptualization. **Jerome Hauselle:** Writing – review & editing, Methodology, Investigation, Formal analysis, Data curation, Conceptualization. **Michael A. Trevino:** Writing – review & editing, Writing – original draft, Project administration, Methodology, Investigation, Formal analysis, Data curation, Conceptualization.

Ethical approval statement

This study was performed in line with the policy statement regarding the use of human subjects by the Helsinki Declaration of 1975, as revised in 2013. Written informed consent and a health and exercise status questionnaire were obtained for all participants. Approval of all experimental procedures was granted by The University Institutional Review Board (protocol number: IRB-20-464-STW).

Declaration of competing interest

The authors declare that they have no known competing financial interests or personal relationships that could have appeared to influence the work reported in this paper.

Acknowledgements

The authors would like to thank all the participants who took time out of their schedules to help with these projects.

References

1. Wormser D, Kaptoge S, Di Angelantonio E, Wood AM, Pennells L, Thompson A. Separate and combined associations of body-mass index and abdominal adiposity with cardiovascular disease: collaborative analysis of 58 prospective studies. *Lancet*. 2011;377(9771):1085–1095. https://doi.org/10.1016/S0140-6736(11)60105-0.
2. Ying-Xiu Z, Shu-Rong W. Secular trends in body mass index and the prevalence of overweight and obesity among children and adolescents in Shandong, China, from 1985 to 2010. *J Public Health*. 2012;34(1):131–137. https://doi.org/10.1093/pubmed/fdr053.
3. Goodpaster BH, Carlson CL, Visser M, et al. Attenuation of skeletal muscle and strength in the elderly: the health ABC study. *J Appl Physiol*. 2001;90(6):2157–2165. https://doi.org/10.1152/jappl.2001.90.6.2157.
4. Thong-Ngam D, Chayanupatkul M, Kittisupamongkon V. Body mass index and percentage of body fat determined physical performance in healthy personnel. *Asian Biomed*. 2012;6(2):313–318. https://doi.org/10.5372/1905-7415.0602.060.
5. Gerber C, Schneeberger AG, Hoppeler H, Meyer DC. Correlation of atrophy and fatty infiltration on strength and integrity of rotator cuff repairs: a study in thirteen patients. *J Shoulder Elb Surg*. 2007;16(6):691–696. https://doi.org/10.1016/j.jse.2007.02.122.
6. Dimmick HL, Miller JD, Sterczala AJ, Trevino MA, Herda TJ. Vastus lateralis muscle tissue composition and motor unit properties in chronically endurance-trained vs. sedentary women. *Eur J Appl Physiol*. 2018;118(9):1789–1800. https://doi.org/10.1007/s00421-018-3909-9.
7. Herda TJ, Ryan ED, Kohlmeier M, Trevino MA, Gerstner GR, Roelofs EJ. Examination of muscle morphology and neuromuscular function in normal weight and overfat children aged 7-10 years. *Scand J Med Sci Sports*. 2018;28(11):2310–2321. https://doi.org/10.1111/sms.13256.
8. Miller JD, Sterczala AJ, Trevino MA, Herda TJ. Examination of muscle composition and motor unit behavior of the first dorsal interosseous of normal and overweight children. *J Neurophysiol*. 2018;119(5):1902–1911. https://doi.org/10.1152/jn.00675.2017.
9. De Luca CJ, LeFever RS, McCue MP, Xenakis AP. Control scheme governing concurrently active human motor units during voluntary contractions. *J Physiol*. 1982;329(1):129–142. https://doi.org/10.1113/jphysiol.1982.sp014294.
10. Ducher G, Bass SL, Naughton GA, Eser P, Telford RD, Daly RM. Overweight children have a greater proportion of fat mass relative to muscle mass in the upper limbs than in the lower limbs: implications for bone strength at the distal forearm. *Am J Clin Nutr*. 2009;90(4):1104–1111. https://doi.org/10.3945/ajcn.2009.28025.
11. Gallagher D, Heymsfield SB, Heo M, Jebb SA, Murgatroyd PR, Sakamoto Y. Healthy percentage body fat ranges: an approach for developing guidelines based on body mass index. *Am J Clin Nutr*. 2000;72(3):694–701. https://doi.org/10.1093/ajcn/72.3.694.
12. Bray G. *Contemporary Diagnosis and Management of Obesity and the Metabolic Syndrome*. fourth ed. Handbooks in Health Care Company; 2003.
13. Colim A, Arezes P, Flores P, Monteiro PRR, Mesquita I, Braga AC. Obesity effects on muscular activity during lifting and lowering tasks. *Int J Occup Saf Ergo*. 2021;27(1): 217–225. https://doi.org/10.1080/10803548.2019.1587223.
14. Baker BS, Chen Z, Larson RD, Bemben MG, Bemben DA. Sex differences in bone density, geometry, and bone strength of competitive soccer players. *J Musculoskelet Neuronal Interact*. 2020;20(1):62–76.
15. Redinger AL, Baker BS. Oral contraceptives and female rowers' skeletal health. *J Strength Condit Res*. 2023;37(3):669. https://doi.org/10.1519/JSC.0000000000004308.
16. Redinger AL, Russell JL, Allen SMF, Baker BS. Height restrictions for dual-energy x-ray absorptiometry: what are our options for body composition and bone health precision? *J Strength Condit Res*. 2024;38(7):e359–e365. https://doi.org/10.1519/JSC.0000000000004775.
17. Baker BS, Li J, Leary EV. DXA2: an automated program for extraction of dual-energy x-ray absorptiometry data. *J Clin Densitom*. 2021;24(4):658–662. https://doi.org/10.1016/j.jocd.2021.02.002.
18. Sterczala AJ, Herda TJ, Miller JD, Ciccone AB, Trevino MA. Age-related differences in the motor unit action potential size in relation to recruitment threshold. *Clin Physiol Funct Imag*. 2018;38(4):610–616. https://doi.org/10.1111/cpf.12453.
19. Mohseny B, Nijhuis TH, Hundepool CA, Janssen WG, Selles RW, Coert JH. Ultrasonographic quantification of intrinsic hand muscle cross-sectional area; reliability and validity for predicting muscle strength. *Arch Phys Med Rehabil*. 2015; 96(5):845–853. https://doi.org/10.1016/j.apmr.2014.11.014.
20. Young HJ, Jenkins NT, Zhao Q, Mccully KK. Measurement of intramuscular fat by muscle echo intensity. *Muscle Nerve*. 2015;52(6):963–971. https://doi.org/10.1002/mus.24656.
21. Herda TJ, Ryan ED, Kohlmeier M, et al. Muscle cross-sectional area and motor unit properties of the medial gastrocnemius and vastus lateralis in normal weight and overfat children. *Exp Physiol*. 2020;105(2):335–346. https://doi.org/10.1113/EP088181.
22. De Luca CJ, Hostage EC. Relationship between firing rate and recruitment threshold of motoneurons in voluntary isometric contractions. *J Neurophysiol*. 2010;104(2): 1034–1046. https://doi.org/10.1152/jn.01018.2009.
23. De Luca CJ, Adam A, Wotiz R, Gilmore LD, Nawab SH. Decomposition of surface EMG signals. *J Neurophysiol*. 2006;96(3):1646–1657. https://doi.org/10.1152/jn.00009.2006.
24. Nawab SH, Chang SS, De Luca CJ. High-yield decomposition of surface EMG signals. *Clin Neurophysiol*. 2010;121(10):1602–1615. https://doi.org/10.1016/j.clinph.2009.11.092.
25. Hu X, Rymer WZ, Suresh NL. Motor unit pool organization examined via spike-triggered averaging of the surface electromyogram. *J Neurophysiol*. 2013;110(5): 1205–1220. https://doi.org/10.1152/jn.00301.2012.
26. Herda TJ, Parra ME, Miller JD, Sterczala AJ, Kelly MR. Measuring the accuracies of motor unit firing times and action potential waveforms derived from surface electromyographic decomposition. *J Electromyogr Kinesiol*. 2020;52:102421. https://doi.org/10.1016/j.jelekin.2020.102421.
27. Sterczala AJ, Miller JD, Dimmick HL, Wray ME, Trevino MA, Herda TJ. Eight weeks of resistance training increases strength, muscle cross-sectional area and motor unit size, but does not alter firing rates in the vastus lateralis. *Eur J Appl Physiol*. 2020; 120(1):281–294. https://doi.org/10.1007/s00421-019-04273-9.
28. Parra ME, Miller JD, Sterczala AJ, Kelly MR, Herda TJ. The reliability of the slopes and y-intercepts of the motor unit firing times and action potential waveforms versus recruitment threshold relationships derived from surface electromyography signal decomposition. *Eur J Appl Physiol*. 2021;121(12):3389–3398. https://doi.org/10.1007/s00421-021-04790-6.
29. Trevino MA, Dimmick HL, Parra ME, et al. Effects of continuous cycling training on motor unit firing rates, input excitation, and myosin heavy chain of the vastus lateralis in sedentary females. *Exp Brain Res*. 2022;240(3):825–839. https://doi.org/10.1007/s00221-021-06278-3.
30. Olmos AA, Sterczala AJ, Parra ME, et al. Sex-related differences in motor unit behavior are influenced by myosin heavy chain during high- but not moderate-intensity contractions. *Acta Physiol*. 2023;239(1):e14024. https://doi.org/10.1111/apha.14024.
31. Farina D, Negro F, Dideriksen JL. The effective neural drive to muscles is the common synaptic input to motor neurons. *J Physiol*. 2014;592(16):3427–3441. https://doi.org/10.1113/jphysiol.2014.273581.
32. Thompson CK, Negro F, Johnson MD, et al. Robust and accurate decoding of motoneuron behaviour and prediction of the resulting force output. *J Physiol*. 2018; 596(14):2643–2659. https://doi.org/10.1113/JP276153.
33. Trevino MA, Herda TJ, Fry AC, et al. Influence of the contractile properties of muscle on motor unit firing rates during a moderate-intensity contraction in vivo. *J Neurophysiol*. 2016;116(2):552–562. https://doi.org/10.1152/jn.01021.2015.
34. Colquhoun RJ, Gai CM, Aguilar D, et al. Training volume, not frequency, indicative of maximal strength adaptations to resistance training. *J Strength Condit Res*. 2018; 32(5):1207. https://doi.org/10.1519/JSC.0000000000002414.
35. Trevino MA, Sterczala AJ, Miller JD, et al. Sex-related differences in muscle size explained by amplitudes of higher-threshold motor unit action potentials and muscle fibre typing. *Acta Physiol*. 2019;225(4):e13151. https://doi.org/10.1111/apha.13151.
36. Parra ME, Sterczala AJ, Miller JD, Trevino MA, Dimmick HL, Herda TJ. Sex-related differences in motor unit firing rates and action potential amplitudes of the first dorsal interosseous during high-, but not low-intensity contractions. *Exp Brain Res*. 2020;238(5):1133–1144. https://doi.org/10.1007/s00221-020-05759-1.

37. Pedhazur EJ. *Multiple Regression in Behavioral Research: Explanation and Prediction*. third ed. Harcourt Brace College Publishers; 1997.
38. Fisher I. The best form of index number. *Q Publ Am Stat Assoc*. 1921;17(133): 533–537. https://doi.org/10.2307/2965310.
39. Hulens M, Vansant G, Lysens R, Claessens AL, Muls E, Brumagne S. Study of differences in peripheral muscle strength of lean versus obese women: an allometric approach. *Int J Obes*. 2001;25(5):676–681. https://doi.org/10.1038/sj.ijo.0801560.
40. Hulens M, Vansant G, Lysens R, Claessens AL, Muls E. Assessment of isokinetic muscle strength in women who are obese. *J Orthop Sports Phys Ther*. 2002;32(7): 347–356. https://doi.org/10.2519/jospt.2002.32.7.347.
41. Lafortuna CL, Maffiuletti NA, Agosti F, Sartorio A. Gender variations of body composition, muscle strength and power output in morbid obesity. *Int J Obes*. 2005; 29(7):833–841. https://doi.org/10.1038/sj.ijo.0802955.
42. Maffiuletti NA, Jubeau M, Munzinger U, et al. Differences in quadriceps muscle strength and fatigue between lean and obese subjects. *Eur J Appl Physiol*. 2007; 101(1):51–59. https://doi.org/10.1007/s00421-007-0471-2.
43. Tomlinson DJ, Erskine RM, Winwood K, Morse CI, Onambélé GL. The impact of obesity on skeletal muscle architecture in untrained young vs. old women. *J Anat*. 2014;225(6):675–684. https://doi.org/10.1111/joa.12248.
44. Paris MT, Letofsky N, Mourtzakis M. Site-specific skeletal muscle echo intensity and thickness differences in subcutaneous adipose tissue matched older and younger adults. *Clin Physiol Funct Imag*. 2021;41(2):156–164. https://doi.org/10.1111/cpf.12679.
45. Freilich RJ, Kirsner RLG, Byrne E. Isometric strength and thickness relationships in human quadriceps muscle. *Neuromuscul Disord*. 1995;5(5):415–422. https://doi.org/10.1016/0960-8966(94)00078-N.
46. Hubal MJ, Gordish-Dressman H, Thompson PD, et al. Variability in muscle size and strength gain after unilateral resistance training. *Med Sci Sports Exerc*. 2005;37(6): 964.
47. Alegre LM, Ferri-Morales A, Rodriguez-Casares R, Aguado X. Effects of isometric training on the knee extensor moment–angle relationship and vastus lateralis muscle architecture. *Eur J Appl Physiol*. 2014;114(11):2437–2446. https://doi.org/10.1007/s00421-014-2967-x.
48. Balshaw TG, Massey GJ, Maden-Wilkinson TM, Tillin NA, Folland JP. Training-specific functional, neural, and hypertrophic adaptations to explosive- vs. sustained-contraction strength training. *J Appl Physiol*. 2016;120(11):1364–1373. https://doi.org/10.1152/japplphysiol.00091.2016.
49. Massey GJ, Balshaw TG, Maden-Wilkinson TM, Tillin NA, Folland JP. Tendinous tissue adaptation to explosive- vs. sustained-contraction strength training. *Front Physiol*. 2018;9:1170. https://doi.org/10.3389/fphys.2018.01170.
50. Farmer SF, Bremner FD, Halliday DM, Rosenberg JR, Stephens JA. The frequency content of common synaptic inputs to motoneurones studied during voluntary isometric contraction in man. *J Physiol*. 1993;470(1):127–155. https://doi.org/10.1113/jphysiol.1993.sp019851.
51. Christie A, Kamen G. Short-term training adaptations in maximal motor unit firing rates and afterhyperpolarization duration. *Muscle Nerve*. 2010;41(5):651–660. https://doi.org/10.1002/mus.21539.
52. Del Vecchio A, Casolo A, Negro F, et al. The increase in muscle force after 4 weeks of strength training is mediated by adaptations in motor unit recruitment and rate coding. *J Physiol*. 2019;597(7):1873–1887. https://doi.org/10.1113/JP277250.
53. Herda TJ, Ryan ED, Kohlmeier M, et al. Muscle cross-sectional area and motor unit properties of the medial gastrocnemius and vastus lateralis in normal weight and overfat children. *Exp Physiol*. 2020;105(2):335–346. https://doi.org/10.1113/EP088181.
54. De Luca CJ, Kline JC. Influence of proprioceptive feedback on the firing rate and recruitment of motoneurons. *J Neural Eng*. 2011;9(1):016007. https://doi.org/10.1088/1741-2560/9/1/016007.